Sensors and Materials, Vol. 38, No. 7 (2026) 4291–4302
MYU Tokyo

S & M 4565

Evaluation of Textile-reinforced-mortar Rehabilitation Performance of Damaged Reinforced Concrete Beam

JungBhin You,[1] Junyoung Byun,[2] and Sungnam Hong[3*]

[1]Department of Civil, Architectural, and Environmental System Engineering, Sungkyunkwan University, 2066 Seobu-ro, Jangan-gu, Suwon-si, Gyeonggi-do 16419, Republic of Korea
[2]Department of Global Smart City, Sungkyunkwan University, 2066 Seobu-ro, Jangan-gu, Suwon-si, Gyeonggi-do 16419, Republic of Korea
[3]Department of Ocean Civil Engineering, Gyeongsang National University, 2-13 Tongyeonghaean-ro, Tongyeong-si, Gyeongsangnam-do 53064, Republic of Korea

(Received December 3, 2025; accepted July 8, 2026)

Keywords: textile-reinforced mortar (TRM), reinforcement, predamaged RC beams, acoustic emission (AE) sensor, flexural performance

In this study, we evaluated the applicability and performance of the textile-reinforced mortar (TRM) reinforcement method to effectively recover the structural performance of the damaged reinforced concrete (RC) beam. Acoustic emission (AE) sensing was employed to monitor damage progression and interfacial behavior during flexural loading. Existing RC structures have deteriorated structural safety owing to aging and damage due to an external environment, and various repair and reinforcement methods have been proposed to compensate for this. In this study, experiments were conducted to evaluate the reinforcement and bending performance of TRM. The actual reinforcement effect was verified by setting the damage load level as a variable. As a result, it was confirmed that TRM reinforcement is effective in restoring the structural performance of damaged RC beams.

1. Introduction

The rapid aging of infrastructure is emerging as a social problem. The long-term use of reinforced concrete (RC) structures and the resultant performance decreases cause deterioration in durability and structural damage. The main causes of deterioration include environmental effects (e.g., salt, freeze-thaw, and carbonation), material problems (decreased concrete quality and rebar corrosion), and increased loads (excessive load and fatigue damage).(1) As a result, damage such as cracking, rebar corrosion, or sheath peeling in RC structures has been reported, and the need for repair and reinforcement is increasing.

Among the existing structure reinforcement methods, the most widely used is the fiber-reinforced polymer (FRP) method. FRP has various advantages such as high strength, light weight, and workability, but has fatal disadvantages such as vulnerability to fire and a high-temperature environment and sensitivity to moisture. As an alternative to overcome these limitations of FRP, there is the textile-reinforced mortar (TRM) method.

*Corresponding author: e-mail: snhong@gnu.ac.kr
https://doi.org/10.18494/SAM6195

ISSN 0914-4935
https://myukk.org/

TRM is a composite reinforcing material that combines an inorganic mortar matrix and high-performance fiber textile. It provides superior fire resistance, environmental resistance, economic feasibility, and construction convenience compared with FRP. TRM can be used even in environments where the existing concrete surface is wet, and durability can be secured even in high-temperature and fire environments.[2–4] It is attracting attention as a repair and reinforcement technology for aging RC structures. Representative preceding studies related to the structural performance review of the TRM reinforcement method were reviewed, and the differentiation of this study and the need for research were summarized.

The most widely used FRP reinforcement method has various advantages such as high strength, light weight, and workability, but has fatal disadvantages such as vulnerability to fire and high-temperature environments and sensitivity to moisture. The TRM method is an alternative to overcome these limitations of FRP.

Dai *et al.* analyzed performance changes in accordance with reinforcement variables such as reinforcement length, the number of fiber layers, and reinforcement position for TRM-reinforced RC beams.[5] The results of their study emphasized that as the reinforcement length increases, the flexural strength and ductility greatly improve, and securing a sufficient attachment length is essential for securing reinforcement performance. D'Ambrisi *et al.* conducted a comparative experiment between the TRM and FRP reinforcement methods to analyze the flexural performance and fracturing characteristics of the structure after TRM reinforcement. As a result of the experiment, the FRP reinforcement showed high initial strength, but there was a risk of brittleness failure, whereas the TRM reinforcement showed excellent performance in terms of crack dispersion and ductility improvement. These results showed that the TRM method can be an excellent alternative in fire resistance, ductility, and environmental resistance compared with the FRP method.[6] Krevaikas conducted an experimental study in which TRM reinforcement was applied to predamaged RC beams, and the number of reinforcement layers, the ratio of reinforcement bars, and the method of arranging reinforcement materials were set as variables. Through the experiment, they confirmed that the strength of the structure can recover up to 99% when TRM was used and reported that the ductility of the structure was improved more than twice after TRM reinforcement. This study is regarded as an early study that proved that TRM reinforcement is effective in improving the structural behavior of damaged structures.[7]

Most of the TRM reinforcement-related studies involved experiments in which the intact state was considered, but from the viewpoint of the actual repair and reinforcement status of old structures, most of the structures were "reinforced without considering the degree of damage to the structure".[8] However, actual on-site structures are exposed to various load and environmental conditions, and damage such as cracks, rebar corrosion, or sheath peeling has already occurred. Previous studies have also emphasized that the existing damage condition of RC members should be considered when evaluating the effectiveness of repair and strengthening methods.[9] When TRM is applied to a structure that is already damaged, various uncertainties such as interfacial adhesion behavior, fiber slip, and peeling exist, so it is necessary to evaluate the effect of TRM reinforcement in accordance with the damaged state.

Koutas *et al.* quantitatively analyzed the load-sagging relationship and destruction mechanism of TRM-reinforced RC beams, and proposed a model that classifies structural behavior step by step. They divided the behavior of TRM-reinforced structures into noncracking sections, sections in which rebar does not yield after cracking, and sections where TRM bears the load after the rebar yield, and presented structural characteristics and design considerations for each step.[10] Giese *et al.* compared and analyzed the structural performance after the TRM reinforcement of RC beams with different degrees of damage. As the predamage load size increased, the yield load and the increase in limit load tended to decrease after TRM reinforcement, which was interpreted as showing that the evaluation of the damage state of the structure is essential during reinforcement design.[11] Du *et al.* developed a TRM reinforcement method that introduced prestressing and applied it to a predamaged RC beam to analyze its effect. As a result of their study, the TRM reinforcement to which prestressing was introduced increased in initial crack load and extreme flexural strength compared with the existing TRM reinforcement, and showed excellent performance in terms of crack control and ductility.[12] Alexander and Shashikala evaluated the carbon textile reinforced geopolymer mortar (CTRGM) reinforcement effect through experiments and numerical analysis on RC beams that were damaged by up to 50–90% of the extreme load. As a result, CTRGM reinforcement significantly improved the performance characteristics of structures, such as flexural strength and ductility, confirming effective performance recovery.[13]

The TRM method has the following technical features compared with the existing structure reinforcement technology. First, TRM is evaluated as a reinforcement technology with excellent fire resistance because it can maintain stable physical performance even under high temperature conditions using mortar, an inorganic matrix.[14] Second, TRM reinforcement technology has advantages in terms of workability and adhesion. TRM is not sensitive to wet conditions, dust, or contamination on the surface of existing concrete structures, and construction is possible even if the surface treatment is simple.[7] This greatly reduces the constraints of the work environment during the repair and reinforcement of actual structures, which is important in increasing on-site workability. Third, fiber textiles in TRM composites effectively redisperse stress even after cracks are generated and suppress the progress of cracks through the crack bridging effect. These characteristics contribute to the improvement of the durability and extended service life of the structure.[6] Fourth, the TRM method can secure both light weight and small thickness at the same time. This feature has the advantage of imposing little additional design load or foundation demand on existing structures. Finally, the TRM reinforcement method has excellent efficiency in terms of economy. In particular, the additional costs incurred from the viewpoint of maintenance and securing long-term durability are relatively small, so the overall life cycle cost reduction effect is evaluated to be very large when applying the actual structure.[14]

Therefore, in our study, we set the degree of damage as a variable on the basis of the analysis and review of existing research trends on the TRM reinforcement method, fiber textile characteristics, and application technology, and TRM reinforcement was performed on test specimens to which the damage load variable was applied to analyze the bending experiment and the behavior of the load–sagging relationship, yield load, and extreme load. Through this, we intend to contribute to realizing the applicability of TRM reinforcement to actual structures and the establishment of design directions for future TRM methods.

2. Materials

TRM composites consist of textiles and a matrix. In addition, the interfacial properties between components have a profound effect on the destruction pattern of the TRM reinforcement and the effect of reinforcing the structure. The textiles constituting the TRM composite material, the matrix, and the interfacial properties thereof have been described.

2.1 Steel

The tensile reinforcement bar (2-D10) was placed at the bottom of the specimen, and D6 stirrups were placed at 100 mm intervals over the entire section to prevent shear failure.

2.2 Textile

In the TRM reinforcement system, the textile is an element that plays the most important role and is mainly manufactured in the form of a fabric using high-performance high-strength fibers. The fibers are arranged in the direction of warp and weft during weaving, and this direction is designed to match the stress transfer path of the structure. The thickness, spacing, number of layers, and weaving method of fibers greatly affect the reinforcement performance, and a design optimized for the required performance is adopted. The textile carries the tensile force of the structure by sharing the crack suppression through continuous stress transfer even after the concrete is cracked. There are various types of fiber used in the TRM method, and the application field may vary depending on each physical property and environmental resistance. Representatively used fibers include carbon, glass, aramid, and basalt fibers.

A high-strength carbon fiber textile was selected for use in the TRM reinforcement method.(15) This reinforcing material has a tensile strength of 4900 MPa and an elastic modulus of 230 GPa. The carbon textile consisted of orthogonally arranged warp and weft rovings with a grid spacing of 10 × 10 mm^2. The rovings were held in position by thermally bonded yarns to maintain the grid geometry during handling and mortar application. For 120-mm-wide beam specimens, the textile was cut to include six longitudinal warp rovings within the strengthening width. The properties of carbon fibers are shown in Table 1.

Table 1
Detailed specifications of carbon textiles (taken from Park(16)).

Properties and geometric parameters	Carbon textile
Tensile strength of filament (MPa)	4900
Modulus of elasticity of filament (GPa)	230
Elongation of filament	0.022
Number of filaments per roving	12000
Diameter of filament (μm)	7
Area per textile (mm^2)	2.772

2.3 Matrix

The concrete used in the production of the test specimen was ready-mixed concrete; the mixing ratio is shown in Table 2, where W/B is the water-to-binder ratio. The design standard compression strength was set to 35 MPa. After 28 days of wet curing after production, the compression strength test was conducted, and as a result, an average compression strength of 40.7 MPa was secured.

Polymeric mortar containing fibers was used as the mortar that produced TRM, and the mixing ratio is shown in Table 3, where W/M is the water-to-mortar ratio. The design reference strength is 45 MPa. Polymeric mortar was also subjected to a compressive strength test after 28 days of wet curing. The compressive strength test was conducted on a cube with a size of $50 \times 50 \times 50$ mm^3 on the basis of ASTM C109. The average compressive strength was 48.6 MPa. Table 4 shows the average compressive strengths of concrete and mortar.

Another important factor affecting the performance of the TRM reinforcement system is the characteristics of the fiber–matrix and matrix–concrete interfaces. The fiber–matrix bond behavior is governed by several factors, including the surface treatment of the fibers, textile architecture, and rheological properties of the matrix. The interfacial adhesion between the matrix and concrete varies depending on whether a primer is applied or the adhesion of the mortar. Table 5 shows the details of the polymer mortar.

Table 2
Mix proportion of concrete.

W/B (%)	Unit weight (kg/m^3)						
	Cement	Water	Fine aggregate	Coarse aggregate	Fly ash	Blast furnace slag	Water reducer
35.8	319	163	780	898	68	68	4.1

Table 3
Mix proportion of mortar.

W/M (%)	Content per 1 bag of 25 kg (%)					
	Cement	Fine aggregate	PVA fiber	Acrylate copolymer	EA	Water reducer
19	319	780	68	68	68	<1

Table 4
Average compressive strengths of concrete and polymer mortar.

Matrix	No. 1 (MPa)	No. 2 (MPa)	No. 3 (MPa)	Average (MPa)
Concrete	42.72	38.12	41.46	40.7
Polymer matrix	48.2	47.4	50.4	48.6

Table 5
Flexural and bond strengths of polymer mortar.

Type	Strength (MPa)	Standard of KS (MPa)
Flexural	8	More than 6
Bond	1.5	More than 1

3. Specimens and Test Setup

3.1 Specimens

The experimental setup was designed to be as similar as possible to the damage situation of the actual structure and the reinforcement environment, and the amount of textile reinforcement was selected on the basis of the results of previous studies.[16]

A total of four beam specimens were fabricated. Two specimens, designated TRM30 and TRM60, were predamaged to predetermined load levels and subsequently strengthened with TRM. The other two specimens were prepared as reference specimens: an unstrengthened RC control specimen and an undamaged TRM-strengthened control specimen. The nominal dimensions of the original RC beam were 1500 mm in length, 120 mm in width, and 135 mm in height. For the strengthened specimens, the total beam height increased to 160 mm after the application of a 25-mm-thick TRM strengthening layer.

Table 6 presents the details of the test specimens and variables. The level of predamage load was set as a variable. Each subject was divided into a no-damage state (0%), a minor-damage state (30%), and an intermediate-damage state (60%) by applying different predamage loads. To ensure that the intended damage levels were achieved, loading was applied under displacement control. Once the target load was reached, the load was removed and the introduction of predamage was terminated. Crack initiation was visually confirmed during loading, and residual deformation was verified on the basis of the remaining displacement after unloading. Three textile sheets were placed in one layer, and the tensile force corresponding to 5% of the tensile strength was introduced for textile linearization. The numbers of textile sheets and layers were fixed at 3 and 1, respectively, and $\rho f/\rho fb$ represents the ratio of the provided textile reinforcement ratio to the balanced textile reinforcement ratio. The RC control specimen without TRM strengthening was specified as RC and the undamaged TRM strengthened control specimen was specified as TRM, and 30 and 60 refer to the test specimens with 30 and 60% of the yield load, respectively.

The TRM reinforcement process was carried out as in the application to an actual structure. Surface treatment was performed on the concrete surface, and then primer application, mortar pouring, textile attachment, and upper mortar pouring finishing were performed in that order. After reinforcement, wet curing was performed for 28 days. The manufacturing process of the experiment is as follows.

(1) After drilling holes at the anchor installation locations, grooves with a depth of 2–3 mm were formed over the entire strengthening surface of the RC beam to improve the bond between the concrete substrate and the TRM layer.

Table 6
Detailed specifications of all specimens.

Specimen	Type	Lamination	Layer	ρ_f/ρ_{fb}	Predamage
RC	RC	—	—	—	—
TRM					—
TRM30	TRM	3	1	64.85%	0.30 P_y
TRM60					0.60 P_y

(2) The RC beams were placed in the formwork prepared for casting the TRM strengthening layer.
(3) The primer was evenly applied to the surface to be strengthened and the anchor was fixed.
(4) The first layer of polymer mortar was applied to a thickness of 12.5 mm.
(5) After placing the reinforcement textile on the poured polymer mortar, a tensile force corresponding to 5% of the textile tensile strength was introduced while the two ends of the textile were fixed.
(6) After placing the textile, additional polymer mortar was applied so that the total thickness of the TRM strengthening layer became 25 mm.
(7) The TRM-strengthened specimens were initially cured in the formwork for one day. After demolding, the specimens were cured at room temperature for an additional 27 days.

3.2 Test setup

The net spacing of the test object was designed to be 1,300 mm, and the pure bending section was designed to be 400 mm at the center. The geometry of the beam specimen, loading configuration, and instrumentation layout are shown in Fig. 1. The load was applied by a 4-point loading method using a 2000 kN universal tester machine (UTM) for displacement control of 0.1 mm/s. One linear variable differential transformer (LVDT) was installed at the center to measure the strain of concrete, and three concrete strain gauges and two rebar strain gauges were installed to check the strain of steel. In addition, four crack gauges with a capacity of 5 mm were attached to measure the strain of TRM and concrete cracks. The acoustic emission (AE) sensor was installed to detect interfacial damage that occurred between the TRM reinforcement and the existing concrete, and the data were used to quantitatively analyze the TRM reinforcement effect and interfacial adhesion state.

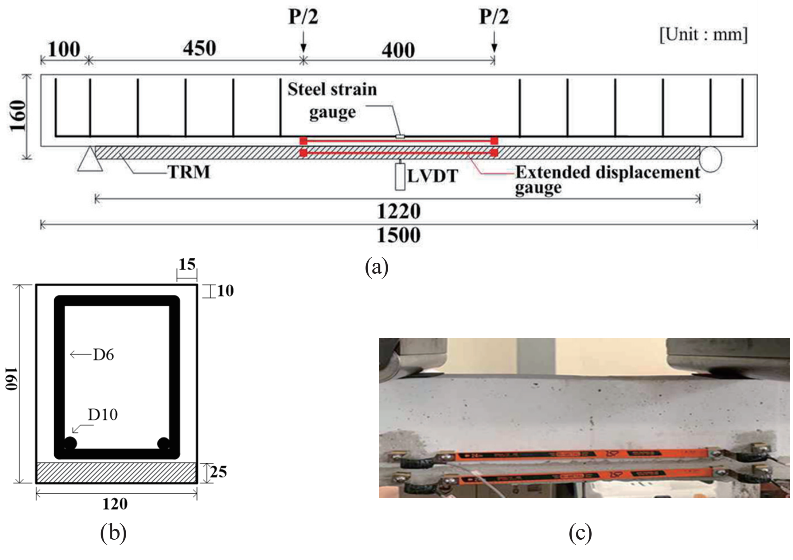

Fig. 1. (Color online) Specifications and test setup of specimens. (a) Front view. (b) Cross-sectional view at center. (c) Extended displacement crack gauge.

4. Experimental Results

Table 7 shows the experimental values of all specimens, and Fig. 2 shows the load-sagging graph of all specimens. The breakdown load and limit load of TRM were 37.92 and 40.75 kN, which increased by 24.65 and 14.95%, respectively, compared with those of RC. The breakdown load and limit load of TRM30 were 38.04 and 40.26 kN, which increased by 25.05 and 13.53% respectively, compared with those of RC. In the case of TRM60, the values were 37.98 and 40.81 kN, which increased by 24.85 and 15.09%, respectively, compared with those of RC. The breakdown load showed the same level of increase, indicating that the reinforcement effect of TRM was secured to a certain level. Under extreme load, the rate of increase was slightly lower than that of the breakdown load, which is because the performance improvement owing to TRM reinforcement in the extreme state is limited owing to the effect of textile and matrix interfacial peeling or slipping.

The loads of TRM, TRM30, and TRM60 were compared. In the case of TRM30, the yield load increased by 0.32% and the limit load decreased by 1.2%. Compared with TRM, the yield load of TRM60 increased by 0.16% and the limit load by 0.15%. When TRM reinforcement was performed on the test subject with less than 60% damage, there was no difference in increase rate, and it was confirmed that the performance of TRM reinforcement was stably maintained. For the same amount of reinforcement within 60% of the yield load, stable reinforcement performance can be secured regardless of the damage rate.

Figure 3 shows the AE hits–time graph. The AE activity exhibited distinct characteristics corresponding to different damage mechanisms. At the early stage of loading, low-amplitude AE

Table 7
Load and deflection of all specimens.

Specimen	Crack		Yield		Ultimate	
	Load (kN)	Def (mm)	Load (kN)	Def (mm)	Load (kN)	Def (mm)
RC	—	—	30.42	9.6	35.46	28.6
TRM	2.59	0.33	37.92	7.84	40.75	11.48
TRM30	2.65	0.35	38.04	8.53	40.26	15.03
TRM60	3.21	0.46	37.98	7.29	40.81	13.8

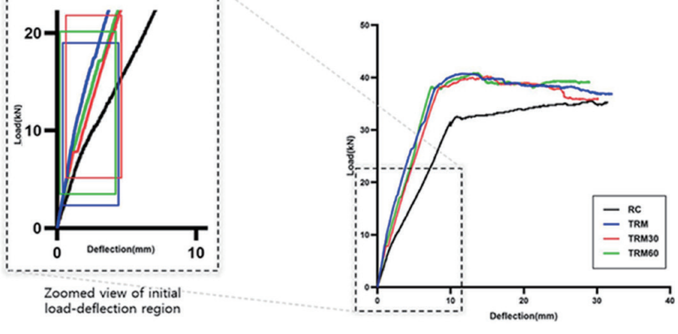

Fig. 2. (Color online) Load–deflection curve.

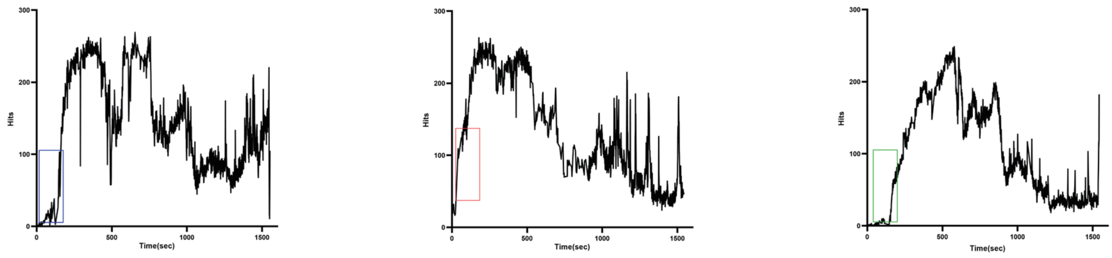

(a) (b) (c)

Fig. 3. (Color online) AE hits–time curve. (a) TRM. (b) TRM30. (c) TRM60.

signals were associated with microcrack initiation within the concrete matrix. As loading progressed, a rapid increase in the number of AE hits was observed, which can be attributed to interfacial slip between the textile and the mortar. At higher load levels, high-energy AE events became dominant, indicating textile rupture and macrocrack propagation. The load at which the initial crack of TRM occurred was 2.59 kN, and an AE signal occurred at about 100 s. After the initial crack, the number of AE hits decreased in the elastic section and then increased rapidly again, which is judged to be the effect of the expansion of the existing crack and the generation of new cracks in the stress redistribution state owing to the resistance of the textile to load and the slip or fracture of the textile that cannot be visually identified.

In the case of TRM30 and TRM60, the loads at which the initial crack occurred were 2.65 and 3.21 kN, respectively, and the AE signal was generated at about 50 and 150 s, as shown in the graph below. After the initial crack, the trend of AE hits was similar to that of TRM. This means that TRM reinforcement suppresses the occurrence of the initial crack and effectively controls the crack progress. However, in the predamaged specimens, most cracks were observed in the existing RC substrate rather than being uniformly distributed by the TRM layer. This behavior may be attributed to the reduced interfacial bond and load-transfer efficiency between the TRM strengthening layer and the existing concrete, because TRM strengthening was applied after predamage had been introduced.(17)

The flexural stiffness is an important performance indicator for assessing serviceability. Therefore, in this section, in order to compare the reinforcement effect in terms of the degree of damage before and after TRM reinforcement, the resistance to the load in the experiment was evaluated by visualizing the flexural stiffness in the form of a graph, as shown in Fig. 4. Flexural stiffness is a factor that indicates the sagging properties of members and is calculated using the following equations using the load and sag measured in the experiment:

$$\delta_c = \frac{P_a a}{24 E_c I_{e,exp}} \left(3a^2 - 4L^2 \right), \tag{1}$$

$$E_c I_{e,exp} = \frac{P_a a}{24 \delta_c} \left(3a^2 - 4L^2 \right). \tag{2}$$

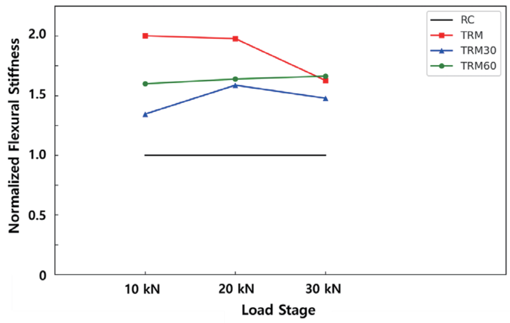

Fig. 4. (Color online) Flexural stiffness ratios of all specimens.

Here, δ_c is the central sag of the simple beam, E_c is the elastic modulus of concrete, $I_{e,exp}$ is the secondary moment of the effective cross section under the total load P, P_a is the load applied at the loading point ($P_a = P/2$), a is the distance from support to the loading point, and L is the clear span between the two supports.

Compared with the RC results, the flexural stiffness of TRM increased by 100, 90, and 62% in the 10, 20, and 30 kN sections, respectively. It can be seen that the improvement of flexural behavior can be expected through TRM reinforcement, and the effect is particularly notable in the initial load section. However, the increase in flexural stiffness became less pronounced as the load increased. This tendency may be attributed to the progressive cracking, interfacial slip, and bond degradation between the TRM layer and the concrete substrate as the structural response became increasingly nonlinear. Therefore, the strengthening effect of TRM was more prominent in the initial loading stage than at higher load levels.(18)

When the flexural stiffness was evaluated at a load level of 10 kN, TRM30 and TRM60 showed reductions of 32% and approximately 20%, respectively, compared with the undamaged TRM-strengthened specimen. When it was 20 kN, TRM30 decreased by 20% and TRM60 decreased by 17%. When it was 30 kN, TRM30 decreased by 9% compared with TRM, but TRM60 increased by 2%. If TRM is reinforced after prior damage, it is highly likely that the interface quality is deteriorated because it is constructed on the surface of concrete where fine cracks and residual deformation have occurred. For this reason, slipping or peeling occurs before TRM sufficiently contributes to the structural behavior, resulting in a marked decrease in flexural stiffness in the early stages of loading.(15,19) Compared with previous studies on intact RC beams strengthened with TRM, the present results demonstrate that predamaged specimens exhibit earlier crack initiation and reduced stiffness. Nevertheless, TRM strengthening remains effective in enhancing load-carrying capacity and crack control, highlighting its applicability under realistic damage conditions.

5. Conclusions

In this study, we evaluated the effect of restoring flexural performance by applying the TRM reinforcement method to a damaged RC beam and analyzed the reinforcement effect in accordance with the damage level. The experiment was conducted on a total of four specimens, and the damage rate was set as a variable for the same amount of reinforcement.

Effective flexural performance recovery was confirmed upon TRM reinforcement. This indicates that the TRM reinforcement improved the overall strength and ductility of the structure through load sharing in the step before the rebar yield. Even in damage within 60% of the yield load, the same level of performance recovery as that of TRM was shown, indicating that performance recovery above a certain level owing to reinforcement is possible at an appropriate time.

The AE data suggest that partial interfacial slip and debonding occurred at the TRM–concrete interface, which may have been affected by the surface quality of the predamaged concrete substrate. This means that if the quality of adhesion between the existing concrete and TRM deteriorates, the reinforcing effect will be reduced.

TRM showed a large flexural stiffness improvement in the initial load section compared with RC, indicating that it can have a positive effect on improving service performance in a limited state of use of the structure. However, as the load increased, the TRM reinforcement effect tended to decrease, which is believed to be due to effects such as decreased interfacial adhesion or slip. In addition, the decrease in the initial section was relatively large, which is believed to be due to microcracks and residual deformation on the damaged concrete surface.

As described above, it was confirmed through experiments that the TRM reinforcement method is effective in restoring the flexural performance of damaged RC beams. With the damage rate within 60% of the yield load at the same reinforcement amount, the TRM reinforcement effect was maintained stably, and this is considered as a reliable performance recovery method for damaged members below a certain level. Furthermore, if the integration of AE sensing and mechanical analysis can be optimized through additional research, it is expected to be an effective approach for identifying damage mechanisms and evaluating the structural performance of TRM-strengthened RC beams.

Acknowledgments

This work was supported by the Gyeongsang National University Fund for Professors on Sabbatical Leave, 2026.

References

1 J. H. Park, S. N. Hong, and S. K. Park: Appl. Sci. **9** (2019) 1981. https://doi.org/10.3390/app9101981
2 S. J. Lee: Doctoral dissertation, Ajou University, Suwon, Korea (2000) (in Korean).
3 S. Yin, S. Xu, and H. Lv: J. Mater. Civ. Eng. **26** (2014) 320. https://doi.org/10.1061/(ASCE)MT.1943-5533.0000811
4 J. H. Park, T. K. Kim, J. B. You, S. Hong, and S. K. Park: J. Korea Inst. Struct. Maint. Insp. **20** (2016) 390 (in Korean).
5 J. Dai, B. Wang, and S. Xu: 2nd Official Int. Conf. Int. Institute for FRP in Construction for Asia-Pacific Region (Seoul, 2009) 75.
6 A. D'Ambrisi, L. Feo, and F. Focacci: Composites, Part B. **44** (2013) 524. https://doi.org/10.1016/j.compositesb.2012.03.011
7 T. D. Krevaikas: Constr. Build. Mater. **208** (2019) 723. https://doi.org/10.1016/j.conbuildmat.2019.03.033
8 J. B. Kim: Master's thesis, Korea National University of Transportation, Chungju, Korea (2018) (in Korean).

9 J. S. Park, K. T. Park, H. B. Park, and B. C. Kim: J. Korea Concr. Inst. **30** (2018) 21. https://www.dbpia.co.kr/journal/articleDetail?nodeId=NODE07504622 (in Korean).
10 L. N. Koutas, Z. Tetta, D. A. Bournas, and T. C. Triantafillou: J. Compos. Constr. **23** (2019) 03118001. https://doi.org/10.1061/(ASCE)CC.1943-5614.0000882
11 A. C. H. Giese, D. N. Giese, V. F. P. Dutra, and L. C. P. Da Silva Filho: J. Build. Eng. **33** (2021) 101873. https://doi.org/10.1016/j.jobe.2020.101873
12 Y. X. Du, X. Shao, S. H. Chu, F. Zhou, and R. K. L. Su: Structures **30** (2021) 735. https://doi.org/10.1016/j.istruc.2021.01.024
13 A. E. Alexander and A. P. Shashikala: Structures **69** (2024) 107522. https://doi.org/10.1016/j.istruc.2024.107522
14 ACI Committee 549: ACI 549.4R-13, Guide to Design and Construction of Externally Bonded Fabric-Reinforced Cementitious Matrix (FRCM) Systems for Repair and Strengthening Concrete and Masonry Structures (American Concrete Institute, Farmington Hills, 2013).
15 S. M. Raoof and D. A. Bournas: Constr. Build. Mater. **154** (2017) 424. https://doi.org/10.1016/j.conbuildmat.2017.07.195
16 J. H. Park: Doctoral dissertation, Sungkyunkwan University, Suwon, Korea (2020) (in Korean).
17 I. S. T. Liu, D. J. Oehlers, and R. Seracino: J. Compos. Constr. **11** (2007) 175. https://doi.org/10.1061/(ASCE)1090-0268(2007)11:2(175)
18 M. U. Hanif, S. Y. Seo, H. V. Tran, and K. Senghong: Dev. Built Environ. **14** (2023) 100141. https://doi.org/10.1016/j.dibe.2023.100141
19 G. Cai, K. D. Tsavdaridis, M. Yoshizawa, and P. Purnell: Proc. Japan Concrete Institute Annual Convention **41** (2019) 1297–1302.

About the Authors

JungBhin You received his B.S. degree from Gangwon University, Republic of Korea, in 2015 and his M.S. and Ph.D. degrees from the Department of Civil, Architectural, and Environmental System Engineering, Sungkyunkwan University, Republic of Korea, in 2020 and 2025, respectively. His research interests are in structural engineering, strengthening, flexural behavior, and textile-reinforced mortar. (94735052@skku.edu)

Jungyung Byun received his B.S. degree from Suwon University, Republic of Korea, in 2024. He is currently pursuing his M.S. degree from the Department of Global Smart City, Sungkyunkwan University, Republic of Korea. His research interests are in structural engineering, strengthening, flexural behavior, and textile-reinforced mortar. (junyoung0629@skku.edu)

Sungnam Hong received his B.S. degree from Sungkyunkwan University, Republic of Korea, in 2003 and his M.S. and Ph.D. degrees from the Department of Civil, Architectural, and Environmental System Engineering, Sungkyunkwan University, in 2005 and 2010, respectively. From 2010 to 2019, he was a research professor at Sungkyunkwan University. Since 2010, he has been a professor at Gyeongsang National University. His research interests are in reinforced concrete and prestressed concrete members. (snhong@gnu.ac.kr)